Maternal germ-line transmission of mutant mtDNAs from embryonic stem cell-derived chimeric mice

James E. Sligh*†‡, Shawn E. Levy†‡, Katrina G. Waymire†, Paulette Allard†, Dirck L. Dillehay§¶, Steven Nusinowitz‖, John R. Heckenlively‖, Grant R. MacGregor†, and Douglas C. Wallace†‖**

†Center for Molecular Medicine, Departments of *Dermatology and §Pathology and ¶Division of Animal Resources, Emory University School of Medicine, 1462 Clifton Road, Atlanta, GA 30322; and ‖Jules Stein Eye Institute, Harbor-UCLA Medical Center, Torrance, CA 90509

Contributed by Douglas C. Wallace, October 16, 2000

We report a method for introducing mtDNA mutations into the mouse female germ line by means of embryonic stem (ES) cell cybrids. Mitochondria were recovered from the brain of a NZB mouse by fusion of synaptosomes to a mtDNA-deficient (ρ^o) cell line. These cybrids were enucleated and the cytoplasts were electrofused to rhodamine-6G (R-6G)-treated female ES cells. The resulting ES cell cybrids permitted transmission of the NZB mtDNAs through the mouse maternal lineage for three generations. Similarly, mtDNAs from a partially respiratory-deficient chloramphenicol-resistant (CAP^R) cell line also were introduced into female chimeric mice and were transmitted to the progeny. CAP^R chimeric mice developed a variety of ocular abnormalities, including congenital cataracts, decreased retinal function, and hamaratomas of the optic nerve. The germ-line transmission of the CAP^R mutation resulted in animals with growth retardation, myopathy, dilated cardiomyopathy, and perinatal or *in utero* lethality. Skeletal and heart muscle mitochondria of the CAP^R mice were enlarged and atypical with inclusions. This mouse ES cell-cybrid approach now provides the means to generate a wide variety of mouse models of mitochondrial disease.

The use of embryonic stem (ES) cells to generate transgenic animals has revolutionized the study of gene action *in vivo* as well as provided animal models for studying pathophysiology and therapies. Strategies for modification of the nuclear genome have become sophisticated, allowing not only for the inactivation of a resident gene, but also for the introduction of more subtle genetic changes, such as the modification of a single base within the genome or modulation of gene expression. Recently, transgenic mouse models for mitochondrial disease have been generated by modifying nuclear-encoded mitochondrial genes (1–6). Although these mice exhibit certain phenotypes characteristic of mitochondrial disease, they cannot recapitulate the unique genetic features of mtDNA mutations, such as maternal inheritance, heteroplasmy, and bioenergetic threshold expression, which are central to understanding mitochondrial diseases (7, 8).

Initial efforts to introduce mtDNA mutations into whole-animal systems have focused on the mtDNAs from cultured mouse cells resistant to the mitochondrial ribosome inhibitor, chloramphenicol (CAP). CAP resistance in a number of mouse cell lines results from a T to C transition at nucleotide pair (np) 2433 {m.2433T>C} near the 3′ end of the 16S rRNA gene (9). Although chimeric mice have been obtained with varying levels of CAP-resistant (CAP^R) and wild-type mtDNAs, a state known as heteroplasmy, transmission through the maternal germ line has not been achieved until recently (10–13).†† This barrier has been overcome in our laboratory by fusion of female mouse ES cells to cytoplasts carrying mutant mtDNAs, and then using the mtDNA mutant ES cells to generate chimeric females that transmit the mtDNA mutations to subsequent generations (11).††

Microinjection of cytoplasm containing foreign mtDNA into oocytes has resulted in chimeric embryos, but the mutant DNA appears to have been rapidly lost by segregation in early preimplantation development (14). Heteroplasmic mice also have been achieved by fusion of cytoplasts to mouse one cell embryos, permitting introduction of mtDNAs with either naturally occurring polymorphisms (15, 16) or deletions (17).

To demonstrate the versatility of the female ES cell cybrid transfer technique for producing transgenic mice with mutant mtDNAs, we now report the introduction and maternal transmission of mtDNAs harboring polymorphic variants or deleterious mutations. This has permitted us to make a more detailed analysis of the transmission of both heteroplasmic and homoplasmic mutations and to assess their *in vivo* consequences. This experimental approach will facilitate production of a variety of mouse models of mtDNA disease.

Methods

ES Cell Culture and Cybrid Preparation. The mouse female CC9.3.1 ES cell line and its derivatives were cultured on mitomycin C-inactivated SNL76/7 feeder cells (18). CC9.3.1 cells were derived from a 129SvEv-*Gpi1*^{c} embryo (A. Bradley, personal communication). Pilot experiments demonstrated that this line would contribute to the female germ line and produce normal fertile females.

To generate female ES cell cybrids, CC9.3.1 cells were plated at a density of 2×10^5 per cm^2, and 24 h later were treated with 0.75 to 1.25 μg/ml of the mitochondrial toxin R-6G (dissolved in 3% ethanol) for up to 72 h. During the R-6G treatment period, the media were supplemented with 1 mM pyruvate and 50 μg/ml uridine. The cells were subsequently washed with PBS and resuspended in 0.3 M mannitol fusion medium for electrofusion.

To recover mtDNAs from the NZB mouse strain, brain synaptosomes were prepared and fused to the mouse ρ^o, thymidine kinase-deficient (TK^-), L cell line LMEB4 (19). LMEB4 (mtNZB) cybrids were selected in 30 μg/ml BrdUrd in the absence of uridine.

To generate donor cytoplasts for the ES cell fusions, either 4×10^7 LMEB4(mtNZB) or 4×10^7 501-1 CAP^R cells (20) were harvested, resuspended in 12.5% Ficoll and 20 μg/ml cytochalasin B, layered onto Ficoll step gradients, and enucleated by centrifugation at 77,000 $\times$ *g* for 1 h at 31°C (21). The cytoplast band was recovered and washed with DMEM, then washed with 0.3 M mannitol fusion medium at pH 7.2. A total of 1×10^7 cytoplasts were mixed with 1×10^6 R-6G-treated ES cells and fused by electric current delivered as a 20-s alignment at 50-V alternate current (AC), followed by two 20-μs pulses of 800-V direct current (DC) (2.5 kV/cm) without a postfusion AC field using a BTX-Genetronics ECM200 (San Diego). After a 2-min

Abbreviations: ES, embryonic stem; CAP, chloramphenicol; np, nucleotide pair; CAP^R, CAP-resistant; TK^-, thymidine kinase-deficient.

‡J.E.S. and S.E.L. contributed equally to this work.

**To whom reprint requests should be addressed. E-mail: dwallace@gen.emory.edu.

††Sligh, J. E., Levy, S. E., Allard, P. M., Waymire, K. G., MacGregor, G. R., Heckenlively, J. R. & Wallace, D. C. (2000) *Am. J. Hum. Genet.* **67,** 19 (abstr.).

The publication costs of this article were defrayed in part by page charge payment. This article must therefore be hereby marked "*advertisement*" in accordance with 18 U.S.C. §1734 solely to indicate this fact.

Article published online before print: *Proc. Natl. Acad. Sci. USA*, 10.1073/pnas.250491597. Article and publication date are at www.pnas.org/cgi/doi/10.1073/pnas.250491597

GENETICS

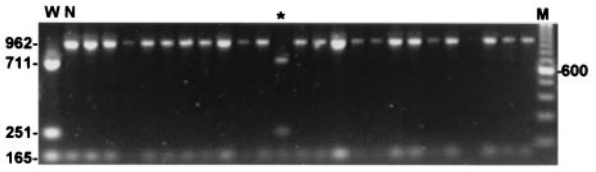

Fig. 1. Genotyping of individual CC9.3.1 (mtNZB) ES cell cybrid clones for NZB mtDNA content using a *Bam*HI mtDNA polymorphism at np 4277. N is the NZB mtDNA. W is the common haplotype (wild type) mtDNA from LM(TK$^-$), the parent cell line of LMEB4. M indicates molecular weight size standards. With the exception of the clone in the lane marked *, the common haplotype was not detected.

recovery time, the cells were plated onto fresh feeders and continued to receive pyruvate and uridine supplementation for 24 h. The cells then were exposed to selection in DMEM with hypoxanthine/aminopterin/thymidine (HAT), without further pyruvate or uridine supplementation. Individual colonies were visible 5 days after fusion and were picked for further expansion and analysis at days 7–9.

Production and Genotyping of Chimeric and Transgenic Mice. Cells that had evidence of the donor cell mtDNA were injected into day 3.5 postcoitum (p.c.) C57BL/6J (B6) blastocysts and the embryos were transferred into day 2.5 p.c. pseudopregnant B6CBAF1 females (22). All experiments using animals were conducted in accordance with the procedures of the Emory University School of Medicine Division of Animal Resources as reviewed by the Emory University Institutional Animal Care and Use Committee and the Research and Education Institute at Harbor-UCLA.

To detect the NZB mtDNA in cybrids and transgenic mice, we took advantage of a naturally occurring *Bam*HI polymorphism. The primers CGGCCCATTCGCGTTATTC and AGGTTGAGTAGAGTGAGGGA were used to PCR-amplify a 1,127-bp fragment over 30 cycles using successive 30-s denaturation (94°C), annealing (55°C), and extension (72°C) steps with *Taq* polymerase (Roche Molecular Biochemicals). The resulting PCR fragment was digested with *Bam*HI (New England Biolabs) and electrophoresed through a 1.7% agarose gel. The NZB mtDNA lacks the *Bam*HI recognition site at np 4277 such that *Bam*HI digestion produces 165- and 962-bp fragments from NZB mtDNAs, but 165-, 251-, and 711-bp fragments from the "common haplotype" mtDNA.

To detect the CAP^R mtDNA, we used a *Tai*I polymorphism generated by the CAP^R mutation. The DNA in the region of the CAP^R mutation was amplified by PCR (23), the 601-bp PCR product was digested with *Tai*I (MBI Fermentas, Amherst, NY), and the fragments were separated through a 1.8% agarose gel.

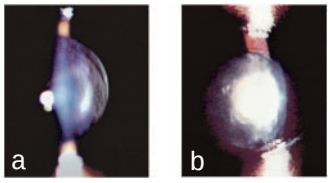

Fig. 3. Slit lamp biomicroscopic examination of CAP^R chimera mouse lens showing cataracts. (*A*) The normal clear lens of a control 129S4 mouse. (*B*) A fetal nuclear cataract of a CAP^R chimera.

CAP^R mtDNAs give a 434-bp fragment, whereas wild-type mtDNAs give a 502-bp fragment.

Pathological Analysis. Tissues were fixed in buffered formalin, embedded in paraffin, sectioned at 6–7 μm, and stained with hematoxylin and eosin. Eyes were removed, immersed in cold 1% paraformaldehyde and 2% glutaraldehyde fixative, washed in Karnovsky buffer, embedded in methacrylate historesin, and sectioned for staining (24).

Electroretinography. After 2 h of dark adaptation, mice were anesthetized by i.p. injection of 15 μg/g Ketamine and 7 μg/g xylazine. Electroretinograms (ERGs) were recorded from the corneal surface of one eye after pupil dilation (1% atropine sulfate) using a gold loop corneal electrode together with a mouth reference and tail ground electrode. Stimuli were produced with a Grass Photic Stimulator (PS33 Plus; Grass Instruments, Quincy, MA) affixed to the outside of a highly reflective Ganzfeld dome. Response signals were amplified (CP511 AC amplifier; Grass Instruments), digitized (PCI-1200; National Instruments, Austin, TX) and computer-analyzed (24).

Rod responses were recorded to short-wavelength (Wratten 47A; λ_{max} = 470 nm) flashes of light over a 3.0-log unit range of intensities (in 0.6-log unit steps) up to the maximum allowable by the photic stimulator (0.668 cd-s/m^2). Mixed rod and cone responses were obtained with white flashes incremented in 0.3-log unit steps up to the maximum allowable (8.46 cd-s/m^2). Cone dominated responses were recorded in response to an intensity series of white flashes (in 0.3 steps) on a rod-saturating background (32 cd/m^2).

To analyze the rod-mediated responses to blue light, the intensity versus *b*-wave amplitude response curves were fitted to the Naka-Rushton function, $V/V_{max} = I/(I + k)$, where V = rod peak-to-peak amplitude, V_{max} = maximum rod amplitude, I = retinal illuminance, and k = retinal illuminance at half amplitude. The rod ERG threshold (2.0 μV criterion) was derived

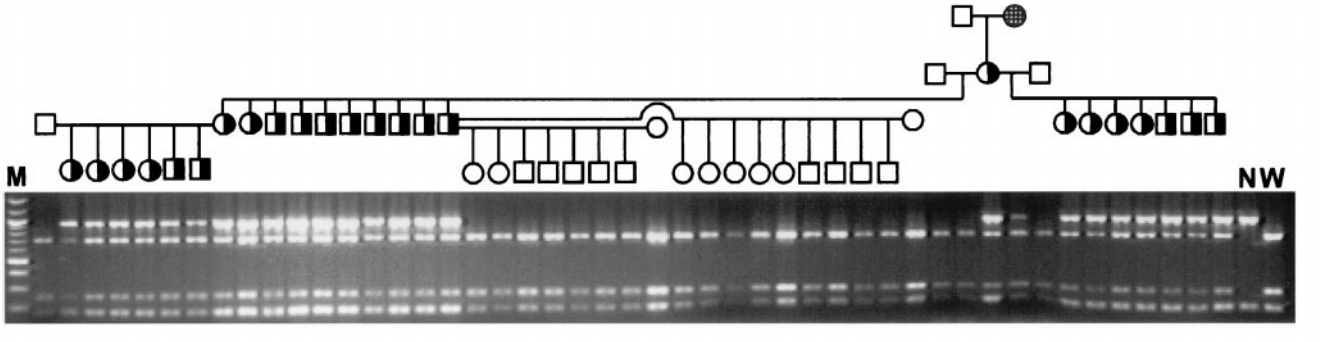

Fig. 2. Introduction of the NZB mtDNA into the female mouse germ line and its maternal inheritance. DNA isolated from tail biopsy tissue was PCR-amplified and digested. The highly chimeric female is indicated by the checkered circle on the top line of the pedigree. She was mated to a B6 male to generate the founding female. Heteroplasmic individuals are represented by half-shaded squares (males) or circles (females). B6 mice were used as mates to test the inheritance of the NZB mtDNA. W is the common haplotype (wild type) mtDNA from the 129SvEv ES cell line CC9.3.1. N is the NZB mtDNA.

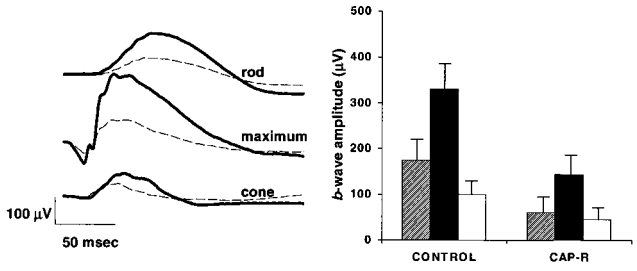

Fig. 4. Electroretinograms of CAP^R chimeric mice. (*A*) Representative responses of rods (*Top*), mixed rods and cones (*Middle*), and cones (*Bottom*) for wild-type 129S4 (solid line) and CAP^R chimeric (dashed line) animals. (*B*) The mean maximum b-wave amplitudes with standard deviation bars for rods (cross hatched bars), mixed rods and cones (filled bars), and cones (open bars) for three representative 129S4 and CAP^R chimeric mice.

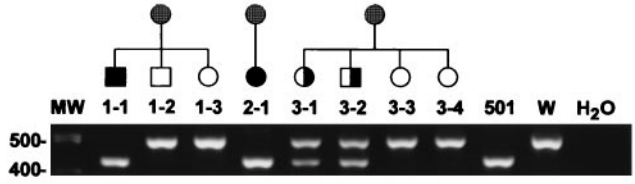

Fig. 6. Germ-line transmission of CAP^R mtDNAs into newborn mice. Chimeric females were mated with B6 males, and tissue DNAs were extracted from offspring. The mtDNA 16S rRNA gene was PCR-amplified and the 601-bp PCR product was digested with *Tai*I. A 434-bp fragment is indicative of CAP^R mtDNAs, whereas a 502-bp fragment size is associated with wild-type mtDNA. MW indicates the molecular weight marker. 1-1, 1–2, and 1–3 are from the first transmitting litter. 2-1 is a pup from a second chimeric female's litter. 3-1, 3-2, 3-3, and 3–4 are from a third chimeric female's litter. 501 is the 501-1 cell line containing CAP^R mtDNA. W is the wild-type mtDNA from the LM(TK$^-$) cell line.

from the Naka-Rushton parameters, such that log threshold = $\log k + 0.3 - \log(V_{max} - 2)$. Similarly, the cone ERG threshold (2.0 μV criterion) was derived from the fit of a linear regression (slope constraint of 1.0) to the intensity-response series obtained to white light on a rod-saturating background.

In these ophthalmological studies, we used 129S4 mice as controls. These differ slightly from the 129SvEv-derived CC9.3.1 cells used to make the chimeras. However, the 129Sv ERG data are representative of that seen for related inbred strains and hence should provide a valid comparison.

Results

Transfer of NZB mtDNA from Brain Tissue into ES Cells. To develop a reliable procedure for introducing exogenous mtDNAs into the mouse germ line, we took advantage of the naturally occurring mtDNA polymorphisms that differentiate mtDNAs of the NZB mouse strain from mtDNAs of most inbred strains that harbor a "common mtDNA haplotype." Inbred mouse strains with the common haplotype (129/Sv, B6, C3H, BALB/c) are thought to have been derived from a single female lineage (25). The NZB and the common haplotype mtDNAs differ by 108 nt, and these polymorphic differences have been used to monitor the segregation of heteroplasmic populations of mtDNAs created by the fusion of cytoplasts from NZB/BINJ with BALB/c single-cell embryos (15, 16).

To establish the NZB mtDNA in cultured mouse L cells, we homogenized the brain of a NZB/BINJ mouse and isolated the synaptosomes by Percoll density gradient centrifugation. The resulting synaptosomes contained one to several mitochondria (19). These synaptosomes were fused by electric field pulse to the ρ° cell line LMEB4 (19). Synaptosome cybrids having the LMEB4 nucleus and the NZB mtDNA [LMEB4 (mtNZB)] were isolated by selection in medium containing BrdUrd but lacking uridine. The LMEB4 (mtNZB) cybrids were then enucleated and the cytoplasts were electrofused to the mouse ES cell line, CC9.3.1.

The CC9.3.1 ES cell line was selected after screening several candidate ES cell lines for the presence or absence of a Y chromosome by PCR of *Sry* (26). CC9.3.1 has a karyotype of 39X, with a normal chromosome G banding pattern (data not shown). Unlike the 45,X Turner syndrome in humans, the 39X karyotype in mouse gives rise to viable and fertile females. Hence, the CC9.3.1 (mtNZB) cybrids have the potential for transmitting the NZB mtDNA through oocytes of the female germ line.

Before cytoplast fusion, the CC9.3.1 cells were depleted of their resident mitochondria by treatment with R-6G. R-6G is a lipophilic mitochondrial poison that inhibits oxidative phosphorylation (OXPHOS), causing an irreversible collapse of

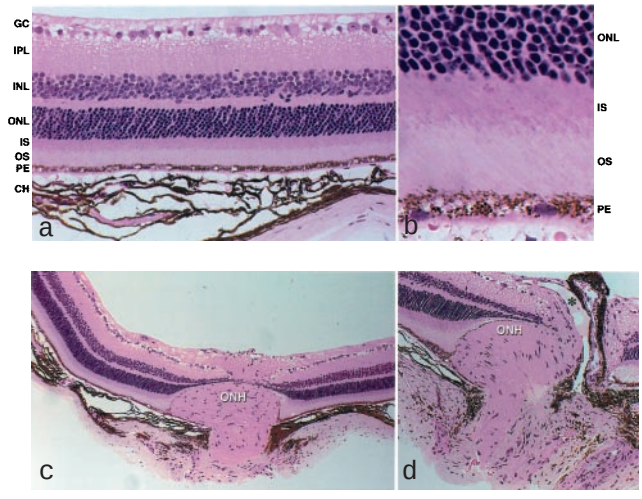

Fig. 5. Retinal light histology of 6-mo-old CAP^R chimeric mice. (*A*) Preservation of retinal layers and a gliotic membrane on the inner retina (Magnified ×400.) (*B*) The pigment epithelial vacuolization and full preservation of outer photoreceptors. (Magnified ×600.) (*C*) The optic nervehead (ONH) light histology demonstrating hamartomatous-like changes intraocularly, with a gliotic membrane emanating from the ONH surface. (Magnified ×200.) (*D*) A similar ONH finding but with the presence of an optic pit (*; magnified ×300) in another CAP^R chimeric mouse. GC = ganglion cell layer, IPL = inner plexiform layer, INL = inner nuclear layer, ONL = outer nuclear layer, IS = inner segment, OS = outer segment of photoreceptors, and PE = pigment epithelium.

Fig. 7. Growth retardation of an agouti mouse harboring CAP^R mtDNA. The 10-day-old agouti pup is shown with four black littermates.

GENETICS

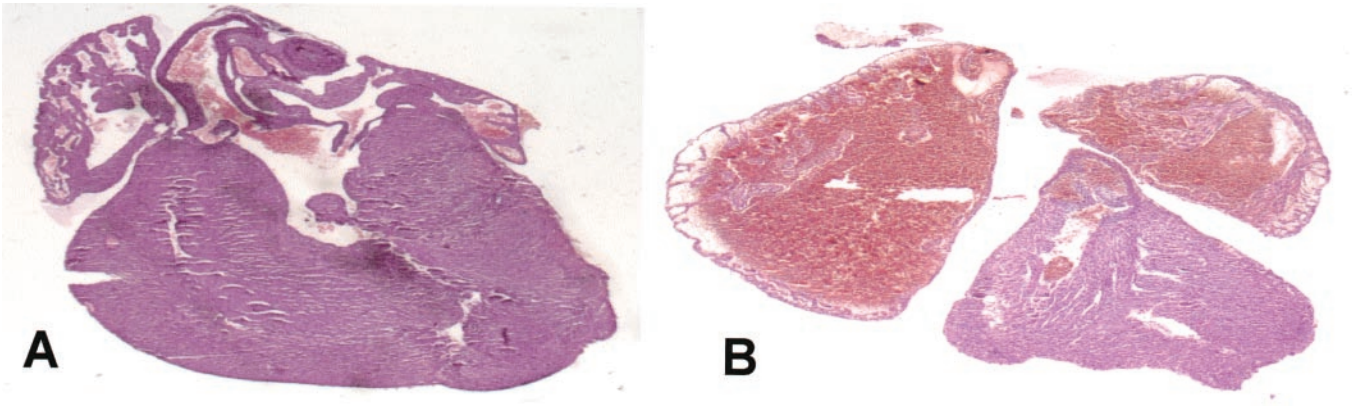

Fig. 8. Dilated cardiomyopathy in a CAP^R neonate on the first day of life. (*A*) A wild-type B6,129S4 control heart. (*B*) The CAP^R neonatal heart.

the mitochondrial membrane potential rendering the cells respiration-deficient (23, 27).

The R-6G-treated CC9.3.1 ES cells were electrofused to LMEB4(mtNZB) cytoplasts and the ES cell cybrids were selected in HAT medium lacking uridine and pyruvate. Individual CC9.3.1 (mtNZB) cybrids were picked and expanded for DNA analysis (28), and the NZB origin of the mtDNA was confirmed by using the polymorphism at np 4277 in the mtDNA ND1 gene. Most cybrids harbored predominantly NZB mtDNAs (Fig. 1).

Generation of mtNZB Transgenic Mice. The CC9.3.1 (mtNZB) ES cell cybrids were injected into B6 blastocysts, and chimeric animals were obtained. Females were mated with B6 males having mtDNAs with the common haplotype and a founder female with the ES cell-encoded agouti coat color was obtained. Mitochondrial genotyping of this animal revealed that she was heteroplasmic, harboring both the NZB and the common haplotype mtDNAs (Fig. 2). Mating this individual with two different B6 males resulted in 7 and 10 offspring, respectively, all of which were heteroplasmic for the NZB and common haplotype mtDNAs. Mating of one of the progeny females with a B6 male again resulted in the maternal transmission of the heteroplasmic mtDNAs. In contrast, no transmission of the heteroplasmic NZB mtDNA was observed in offspring after mating of a heteroplasmic male with two different B6 females (Fig. 2). Analysis of mtDNA in multiple tissues derived from all three germ layers (ectoderm, mesoderm, and endoderm) revealed heteroplasmy throughout the animals. None of the heteroplasmic mice had an overtly abnormal phenotype. Thus, the NZB mtDNA, recovered in cultured mouse L cells from NZB mouse brains, was successfully introduced into the mouse female germ line by using ES cells and maternally transmitted through multiple generations.

Transfer of the CAP^R Mutation into ES Cells. To confirm the generality of this ES cell cybrid methodology to generate transgenic mice with altered mtDNA, we repeated this process by using the CAP^R mtDNA mutation of mouse 501-1 cells. The CAP^R mutation creates a *Tai*I restriction site in the mtDNA 16S rRNA gene and renders the cells partially respiratory deficient (11). The CC9.3.1 cell line was cured of its resident mitochondria by treatment with R-6G, fused to the cytoplasts from enucleated 501-1 cells. The cybrids were selected in medium containing HAT but without uridine. Most of the resulting CC9.3.1 (mt501-1) ES cell cybrids were homoplasmic for the CAP^R mtDNA and were capable of continued growth on CAP^R SNL76/7 feeder cells in the presence of 50 μg/ml CAP for at least 4 wk. CC9.3.1 cells without CAP^R mtDNAs ceased growing within 7 days of exposure to 50 μg/ml CAP. Multiple CC9.3.1 (mt501-1) cybrids were injected into B6 blastocysts and chimeric mice were obtained. The animals discussed in this paper were derived from cybrid clones CB9 and CB11.

CAP^R Chimeric Mouse Ophthalmological Phenotype. Phenotypic examination of chimeric mice with predominantly agouti coat color contributed from the CAP^R ES cells revealed the presence of congenital cataracts. These cataracts were apparent when the mice opened their eyes in the second week of life. All mice had bilateral cataracts, but variable opacity was observed. The cataracts were fetal nuclear in location, consistent with cataracts seen in other mice strains with crystalline gene mutations (29, 30). In most cases, the fetal nucleus of the lens had a dense opacity, and in some mice the opacities extended into the cortex. These cataracts were observed in mice derived from multiple independent clones harboring the CAP^R mtDNA, but never from the clones containing NZB mtDNA. A typical nuclear cataract of a CAP^R mouse together with a control, as revealed by slit lamp biomicroscopy, is shown in Fig. 3.

To determine whether the presence of CAP^R cells affected retinal function, we performed ERGs on 19 CAP^R chimeric, CB11-derived, male mice with substantial agouti coat color. These were compared with six 129S4 controls. Representative ERGs for the CAP^R chimeric and 129S4 control mice are shown in Fig. 4*A*. ERG b-wave amplitudes for the chimeric mice were reduced 50–60% with respect to the controls, with both rods and cones being similarly affected (Fig. 4*B*). The timing of peak responses was similar for the two groups of mice, although there was a trend for prolonged latencies for the CAP^R chimeric mice.

To further characterize the intensity-response series of both rods and cones, the blue and white flash series were fitted to the Naka-Rushton function. For the rods (blue-intensity series) the maximum saturated b-wave response (V_{max}) of the CAP^R chimeras was an average of 0.40 log units smaller than that of the 129S4 control mice; the rod ERG threshold intensity was elevated by 0.51 log units in the CAP^R chimeric mice, and the retinal illuminance at half amplitude (k) was elevated by 0.003 log units. Similarly, the cone ERG threshold intensity of the CAP^R chimeras was elevated 0.37 log units as compared with the control 129S4 mice.

Although both a- and b-waves were decreased in the CAP^R chimeric mice, there was a generally greater deficit in the b-wave. To explore this further, the a- to b-wave amplitude ratio, b/a, was calculated for each mouse eye. The b/a ratio ($\pm$1 SD) was 2.6 $\pm$ 0.4 for the CAP^R chimeras and 3.6 $\pm$ 0.7 for the 129S4 controls. Hence, there is a marked decrease in the b-wave amplitude, indicating that the CAP^R chimeras have a marked reduction in both rod and cone function.

Histology of CAP^R Mutants. The light microscopy retinal histology was normal in the CAP^R chimeric CB11 mice, and no evidence of

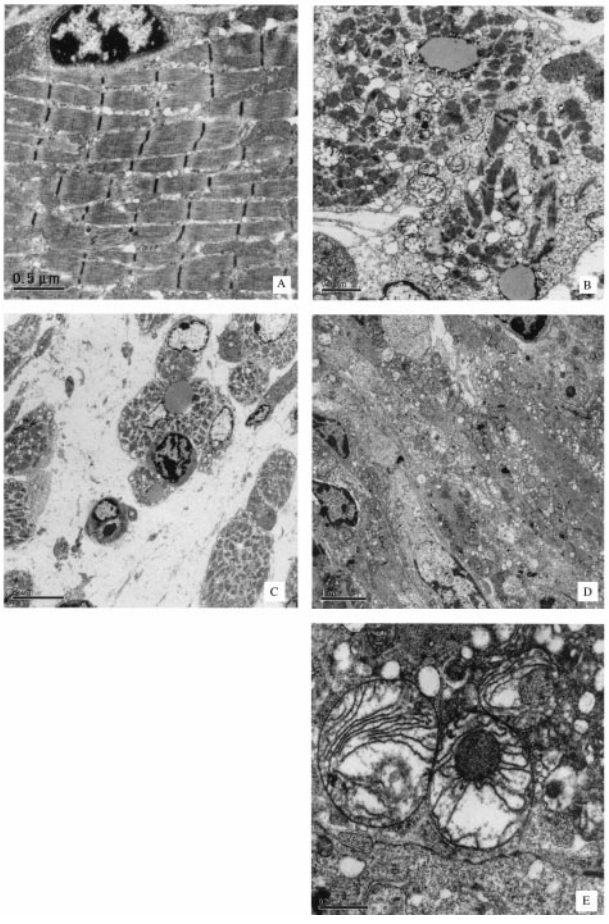

Fig. 9. Ultrastructural abnormalities of CAP^R mouse skeletal muscle and heart. (*A–C*) Skeletal muscle samples. (*D* and *E*) Heart. (*A*) Wild-type control skeletal muscle at ×4,400. (*B–E*) CAP^R mutant specimens, *B* at ×3,400, *C* at ×1,100, *D* at ×1,950, and *E* at ×10,500.

retinal degeneration was observed despite the ERG amplitude loss of rods and cones. The pigment epithelium (PE) showed vacuoles throughout on all CAP^R chimeric specimens examined (Fig. 5*A*). However, the most striking abnormality was hamartomatous-like changes of the optic nervehead, whose substance protrudes into the intraocular space (Fig. 5*B*). A gliotic membrane emanating from the surface of the optic nervehead covered the inner retinal surface (Fig. 5*C*).

Germ-Line Transmission and Lethality of the CAP^R Mutation. Chimeric females generated from two independent CC9.3.1 (mt501-1) cybrid clones transmitted the CAP^R mutation to their progeny. The genotypes of the first four mice born harboring the CAP^R mutation in all of the cells of the body are shown in Fig. 6. Both homoplasmic (Fig. 6, 1-1 and 2-1) and heteroplasmic (Fig. 6, 3-1 and 3-2) CAP^R mice were born. Of the two heteroplasmic pups, pup 3-1 harbored 44% and pup 3-2 harbored 52% CAP^R mtDNAs, as measured in tail tissue biopsy.

The mutant mice showed marked growth retardation at birth. The average weight of the newborn homoplasmic mutant pups was 0.9 g compared with 1.4 g for mice born in our facility with identical nuclear backgrounds. Moreover, with the exception of pup 2-1, all mice born with CAP^R mtDNA died within the first 12 h of birth.

Genotypic analysis of embryos recovered from pregnant chimeric females revealed that additional CAP^R animals died *in utero*. Growth-retarded, necrotic embryos, homoplasmic for the CAP^R mutation, were observed at both embryonic day 15.5 and 17.5.

A single CAP^R pup (2-1) survived beyond the first day of life. This pup was notably smaller than the other littermates at birth (Fig. 7). Although the development of hair was delayed, this pup ultimately developed the agouti hair color derived from CC9.3.1 ES cells. The pup continued to exhibit severe growth retardation throughout life and died at 11 days of age, having a weight of only 2.3 g compared with a mean weight of 6 g for four littermates.

Myopathy and Cardiomyopathy in CAP^R Mutant Mice. Mutant mice displayed a variety of degenerative changes in both skeletal muscle and heart on gross and microscopic examination. The skeletal muscle from CAP^R pups revealed severe mitochondrial myopathy. Light microscopy revealed degenerative changes and striking loss of muscle fibers and highly abnormal mitochondria. The pathological analysis of the heart of a CAP^R neonate, examined 6 h after birth, revealed a dramatic dilated cardiomyopathy. Thinning of the atrial walls, and a marked enlargement of the atria, was observed with the atria exceeding the volume of the normally larger ventricles (Fig. 8).

Ultrastructural analysis confirmed the skeletal muscle and heart pathology. The skeletal muscle showed marked muscle fiber degeneration. Normal muscle cells have highly organized contractile arrays with mitochondria arranged at regular intervals adjacent to Z bands (Fig. 9*A*). By contrast, in the mutant muscle, there was a striking proliferation of mitochondria which splayed, displaced, or replaced contractile elements and 0.5- to 1-μm inclusions were observed within the cells (Fig. 9*B*). Some muscle fibers appeared as "ghost" cells in which only the nucleus and filament remnants occupied the intracellular space. The prevalence of gaps within the muscle indicated that many muscle fiber cells had been completely lost (Fig. 9*C*). Abnormal enlarged mitochondria were prominent and contained internal annular bodies and electron dense granules.

Ultrastructure analysis of the heart revealed a paucity of normal sarcomeres and an abundance of atypical mitochondria (Fig. 9*D*). There was a proliferation of abnormal mitochondria, some of which were enlarged and others had internal inclusion bodies (Fig. 9*E*).

In summary, the CAP^R mtDNA was transmitted through the female germ line and some animals with a significant proportion of CAP^R mtDNA developed to term. However, the presence of this mutation was incompatible with life beyond the neonatal period. The severe mitochondrial myopathy and cardiomyopathy observed in the CAP^R mouse is reminiscent of the phenotype seen in humans with the most severe mtDNA protein synthesis mutations (8).

Discussion

We have introduced two different mtDNAs from cultured mouse cell lines into the mouse female germ line: one derived from the synaptosomes of a NZB mouse and another from a CAP^R mouse cell line. Although the mice with the NZB mtDNAs appeared normal, those with the CAP^R mtDNAs produced a phenotype not only in the germ-line progeny, but also in the chimeric parents.

The CAP^R chimeras developed an ocular phenotype including congenital cataracts and functional retinopathy. This is reminiscent of the retinal defects seen in humans with mtDNA disease. For example, a portion of Kearn–Sayres syndrome patients have mild loss of ERG function with granular subretinal pigmentary changes on ophthalmoscopy (31). Retinitis pigmentosa and macular degeneration have been also observed in patients harboring the heteroplasmic T8993G ATP6 gene mtDNA mutation (32) and retinitis pigmentosa, cataracts, and glaucoma have been reported in a patient with a heteroplasmic np 2971T deletion, which disrupts the anticodon loop of the tRNA$^{Leu(UUR)}$ (33).

It is currently unknown why the CAP^R mutation induces cataract formation. The lens is a highly complex structure consisting of numerous types of crystalline proteins that form the lens sequentially during development (34). It is possible that an

energetic defect alters the development of the lens fibers during the fetal stage of lens development. The CAP^R mutation also could result in increased mitochondrial production of reactive oxygen species throughout the development of the early eye altering the lens crystalline proteins, as has been suggested for the formation of cataracts in the elderly.

The functional retinopathy, associated with the depression of both rod and cone function and degenerative changes in the retinal pigment epithelium, suggests a metabolic defect as there is no evidence of degeneration of the photoreceptor cells. Loss of ERG amplitude in mouse models normally is associated with obvious proportionate degeneration of the retina on histology. However, the ERG findings in the CAP^R mice may be similar to the alterations in retinal function seen in patients who harbor the NARP G9883T ATPase6 gene mutation (35).

The growth retardation of the CAP^R mice is associated with mitochondrial cardiomyopathy and myopathy, analogous to that observed in a large human family harboring a high percentage of the $tRNA^{Leu(UUR)}$ A3243G MELAS mutation. The mother of the family showed lactic acidosis and growth retardation. She had 11 children, who also exhibited lactic acidosis and growth retardation, most of which died in their teens or 20s of either cardiomyopathy or status epilepticus (36). Hence, the CAP^R mice seem to represent a more severe form of some of the classical manifestations of mtDNA protein synthesis mutations.

With our method, it will now be feasible to introduce a wide variety of mouse mtDNAs into the mouse female germ line via somatic cell genetics. These could be naturally occurring variants from different strains or species of mice and rodents or additional mutants resistant to mitochondrial OXPHOS inhibitors such as rotenone, antimycin A, and mycidin (13, 37–41). In addition, the recovery of somatic mtDNA mutants that accumulate during normal aging by clonal expansion of brain mtDNAs in synaptosome cybrids (19) also may permit the introduction of naturally occurring deleterious somatic mtDNA mutations into mice. Such transgenic mice would allow the exploration of mtDNA changes in complex genetic processes such as aging.

We thank Dr. Allan Bradley for graciously contributing the CC9.3.1 cell line, Dr. Kevin Winn for pathological consultation, Dr. Asif M. Azimi for collection of the ERG and cataract data, and Ms. Marie T. Lott for assistance in preparing this manuscript and bioinformatics support. J.E.S. is a Howard Hughes Medical Institute Physician Postdoctoral Fellow, and J.R.H. is the recipient of a Senior Scientist Award from Research to Prevent Blindness. This work was funded by National Institutes of Health R01 Grants NS21328, HL45572, and AG13154 (to D.C.W.), HD36437 (to G.R.M.), and EY7752 (to J.R.H.).

1. Li, Y., Huang, T. T., Carlson, E. J., Melov, S., Ursell, P. C., Olson, J. L., Noble, L. J., Yoshimura, M. P., Berger, C., Chan, P. H., *et al.* (1995) *Nat. Genet.* **11,** 376–381.
2. Graham, B., Waymire, K., Cottrell, B., Trounce, I. A., MacGregor, G. R. & Wallace, D. C. (1997) *Nat. Genet.* **16,** 226–234.
3. Melov, S., Schneider, J. A., Day, B. J., Hinerfeld, D., Coskun, P., Mirra, S. S., Crapo, J. D. & Wallace, D. C. (1998) *Nat. Genet.* **18,** 159–163.
4. Melov, S., Coskun, P., Patel, M., Tunistra, R., Cottrell, B., Jun, A. S., Zastawny, T. H., Dizdaroglu, M., Goodman, S. I., Huang, T., *et al.* (1999) *Proc. Natl. Acad. Sci. USA* **96,** 846–851.
5. Esposito, L. A., Kokoszka, J. E., Waymire, K. G., Cottrell, B., MacGregor, G. R. & Wallace, D. C. (2000) *Free Radical Biol. Med.* **28,** 754–766.
6. Larsson, N. G., Wang, J., Wilhelmsson, H., Oldfors, A., Rustin, P., Lewandoski, M., Barsh, G. S. & Clayton, D. A. (1998) *Nat. Genet.* **18,** 231–236.
7. Wallace, D. C. (1999) *Science* **283,** 1482–1488.
8. Wallace, D. C., Brown, M. D. & Lott, M. T. (1996) in *Emery and Rimoin's Principles and Practice of Medical Genetics*, eds. Rimoin, D. L., Connor, J. M., Pyeritz, R. E. & Emery, A. E. H. (Churchill Livingstone, London), Vol. 1, pp. 277–332.
9. Blanc, H., Adams, C. W. & Wallace, D. C. (1981) *Nucleic Acids Res.* **9,** 5785–5795.
10. Watanabe, T., Dewey, M. J. & Mintz, B. (1978) *Proc. Natl. Acad. Sci. USA* **75,** 5113–5117.
11. Levy, S. E., Waymire, K. G., Kim, Y. L., MacGregor, G. R. & Wallace, D. C. (1999) *Transgenic Res.* **8,** 137–145.
12. Marchington, D. R., Barlow, D. & Poulton, J. (1999) *Nat. Med.* **5,** 957–960.
13. Bai, Y. & Attardi, G. (1998) *EMBO J.* **17,** 4848–4858.
14. Pinkert, C. A., Irwin, M. H., Johnson, L. W. & Moffatt, R. J. (1997) *Transgenic Res.* **6,** 379–383.
15. Jenuth, J. P., Peterson, A. C., Fu, K. & Shoubridge, E. A. (1996) *Nat. Genet.* **14,** 146–151.
16. Jenuth, J. P., Peterson, A. C. & Shoubridge, E. A. (1997) *Nat. Genet.* **16,** 93–95.
17. Inoue, K., Nakada, K., Ogura, A., Isobe, K., Goto, Y., Nonaka, I. & Hayashi, J.-I. (2000) *Nat. Genet.* **26,** 176–181.
18. McMahon, A. P. & Bradley, A. (1990) *Cell* **62,** 1073–1085.
19. Trounce, I., Schmiedel, J., Yen, H. C., Hosseini, S., Brown, M. D., Olson, J. J. & Wallace, D. C. (2000) *Nucleic Acids Res.* **28,** 2164–2170.
20. Bunn, C. L., Wallace, D. C. & Eisenstadt, J. M. (1974) *Proc. Natl. Acad. Sci. USA* **71,** 1681–1685.
21. Stocco, D. M. (1983) *Anal. Biochem.* **131,** 453–457.
22. Bradley, A. (1987) in *Teratocarcinomas and Embryonic Stem Cells. A Practical Approach*, ed. Robertson, E. J. (IRL Press, Oxford), pp. 113–151.
23. Trounce, I. & Wallace, D. C. (1996) *Somat. Cell Mol. Genet.* **22,** 81–85.
24. Akhmedov, N. B., Piriev, N. I., Chang, B., Rapoport, A. L., Hawes, N. L., Nishina, P. M., Nusinowitz, S., Heckenlively, J. R., Roderick, T. H., Kozak, C. A., *et al.* (2000) *Proc. Natl. Acad. Sci. USA* **97,** 5551–5556.
25. Ferris, S. D., Sage, R. D. & Wilson, A. C. (1982) *Nature (London)* **295,** 163–165.
26. Koopman, P., Gubbay, J., Vivian, N., Goodfellow, P. & Lovell-Badge, R. (1991) *Nature (London)* **351,** 117–121.
27. Gear, A. R. (1974) *J. Biol. Chem.* **249,** 3628–3637.
28. Ramirez-Solis, R., Rivera-Perez, J., Wallace, J. D., Wims, M., Zheng, H. & Bradley, A. (1992) *Anal. Biochem.* **201,** 331–335.
29. Chang, B., Hawes, N. L., Roderick, T. H., Smith, R. S., Heckenlively, J. R., Horwitz, J. & Davisson, M. T. (1999) *Mol. Vis.* **5,** 21.
30. Smith, R. S., Hawes, N. L., Chang, B., Roderick, T. H., Akeson, E. C., Heckenlively, J. R., Gong, X., Wang, X. & Davisson, M. T. (2000) *Genomics* **63,** 314–320.
31. Ota, Y., Miyake, Y., Awaya, S., Kumagai, T., Tanaka, M. & Ozawa, T. (1994) *Retina* **14,** 270–276.
32. Ortiz, R. G., Newman, N. J., Shoffner, J. M., Kaufman, A. E., Koontz, D. A. & Wallace, D. C. (1993) *Arch. Ophthalmol.* **111,** 1525–1530.
33. Shoffner, J. M., Bialer, M. G., Pavlakis, S. G., Lott, M. T., Kaufman, A., Dixon, J., Teichberg, S. & Wallace, D. C. (1995) *Neurology* **45,** 286–292.
34. McAvoy, J. W., Chamberlain, C. G., de Iongh, R. U., Hales, A. M. & Lovicu, F. J. (1999) *Eye* **13,** 425–437.
35. Chowers, I., Lerman-Sagie, T., Elpeleg, O. N., Shaag, A. & Merin, S. (1999) *Br. J. Ophthalmol.* **83,** 190–193.
36. Heddi, A., Stepien, G., Benke, P. J. & Wallace, D. C. (1999) *J. Biol. Chem.* **274,** 22968–22976.
37. Howell, N., Bantel, A. & Huang, P. (1983) *Somatic Cell Genet.* **9,** 721–743.
38. Howell, N., Huang, P., Kelliher, K. & Ryan, M. L. (1983) *Somatic Cell Genet.* **9,** 143–163.
39. Howell, N., Appel, J., Cook, J. P., Howell, B. & Hauswirth, W. W. (1987) *J. Biol. Chem.* **262,** 2411–2414.
40. Howell, N. & Gilbert, K. (1988) *J. Mol. Biol.* **203,** 607–618.
41. Howell, N. (1990) *Biochemistry* **29,** 8970–8977.